

AperTO - Archivio Istituzionale Open Access dell'Università di Torino

Rayleigh-Taylor turbulence with singular nonuniform initial conditions

This is a pre print version of the following article:

Original Citation:

Availability:

This version is available <http://hdl.handle.net/2318/1676459> since 2018-09-12T21:21:35Z

Published version:

DOI:10.1103/PhysRevFluids.3.092601

Terms of use:

Open Access

Anyone can freely access the full text of works made available as "Open Access". Works made available under a Creative Commons license can be used according to the terms and conditions of said license. Use of all other works requires consent of the right holder (author or publisher) if not exempted from copyright protection by the applicable law.

(Article begins on next page)

Rayleigh-Taylor turbulence with singular non-uniform initial conditions

L. Biferale,¹ G. Boffetta,² A.A. Mailybaev,³ and A. Scagliarini⁴

¹*Department of Physics and INFN, Rome*

²*Department of Physics and INFN, University of Torino, via P. Giuria 1, 10125 Torino, Italy*

³*Instituto Nacional de Matemática Pura e Aplicada – IMPA, 22460-320 Rio de Janeiro, Brazil*

⁴*Istituto per le Applicazioni del Calcolo ‘M. Picone’ – IAC-CNR, Via dei Taurini 19, 00185 Rome, Italy*

We perform Direct Numerical Simulations of three dimensional Rayleigh-Taylor turbulence with a non-uniform singular initial density/temperature background. In such conditions, the mixing layer evolves under the driving of a varying effective Atwood number; the long time growth is still self-similar, but not anymore proportional to t^2 and depends on the singularity exponent c of the initial profile $\Delta T \propto z^c$. We show that the universality is recovered when looking at the *efficiency*, defined as the ratio of the variation rates of the kinetic energy over the heat flux. A closure model is proposed that is able to reproduce analytically the time evolution of the mean temperature profiles, in excellent agreement with the numerical results. Finally, we reinterpret our findings on the light of *spontaneous stochasticity* where the growth of the mixing layer is mapped in to the propagation of a wave of turbulent fluctuations on a rough background.

INTRODUCTION. Turbulent mixing is a mechanism of utmost importance in many natural and industrial processes, often induced by the Rayleigh-Taylor (RT) instability which takes place when a fluid is accelerated against a less dense one [1–5]. RT turbulence occurs in disciplines as diverse as astrophysics [6–8], atmospheric science [9] or confined nuclear fusion [10, 11] (see [4, 5] for recent reviews).

One important application of RT instability is the case of convective flow, in which density differences reflect temperature fluctuations of a single fluid and the acceleration is provided by gravity. In the simplest configuration, RT turbulence considers a planar interface which separates a layer of cooler (heavier, of density ρ_H) fluid over a layer of hotter (lighter, of density ρ_L) fluid under a constant body force such as gravity. The driving force is constant in time and proportional to $g\mathcal{A}$, where g is the acceleration due to the body force and $\mathcal{A} = (\rho_H - \rho_L)/(\rho_H + \rho_L) = \beta\theta_0/2$ is the Atwood number, expressed in term of the thermal expansion coefficient β and the temperature jump θ_0 between the two layers. However, in some relevant circumstances one has to cope with time varying acceleration (as in inertial confinement fusion or in pulsating stars [12–14]) or with a varying Atwood number, that emerges when the mixing proceeds over a non-uniform background as in thermally stratified atmosphere [15–17].

In this Letter we address a question with both fundamental and applied importance: what happens when the initial unstable background has a non-trivial singular profile. In particular we investigate analytically and by using direct numerical simulations in three dimensions the generic case when the initial unstable vertical temperature distribution is given by a power law:

$$T_0(z) = -(\theta_0/2) \operatorname{sgn}(z) \left(\frac{|z|}{L}\right)^c, \quad (1)$$

where L is characteristic length scale ($-L \leq z \leq L$).

The exponent of the singularity belongs to the interval $-1 < c < 1$, where the upper limit corresponds to a smooth profile and the lower limit ensures that the potential energy, $-\beta g z T_0(z)$, does not diverge near the interface among the two miscible fluids at $z = 0$. The limit $c = 0$ recovers the standard RT configuration.

We develop a closure model based on the Prandtl Mixing Length approach, which is able to predict with good accuracy the evolution of the RT turbulence at all scales and for all values of the singularity exponent c . Beside the importance of testing the robustness with respect to the initial configuration, the above setup allows us to investigate the idea that the Mixing Layer (ML) growth can be mapped to a traveling wave in appropriate renormalized variables. This wave describes the self-similar evolution of the probability distribution function (PDF) of turbulent fluctuations from small to large scales in a rough background given by the initial singular profile [18, 19]. Such a description would then naturally explain the universality of the ML evolution and its spontaneously stochastic behavior in the inertial range [20]. We introduce a shell model for the RT evolution to illustrate and quantify the ML statistical properties.

RESULTS FOR NAVIER–STOKES EQUATIONS. We consider the Navier-Stokes equation for the incompressible velocity field $\mathbf{u}(\mathbf{r}, t)$ with Boussinesq buoyancy term and the coupled equation for the temperature field $T(\mathbf{r}, t)$:

$$\partial_t \mathbf{u} + \mathbf{u} \cdot \nabla \mathbf{u} = -\nabla p + \nu \nabla^2 \mathbf{u} - \beta g T, \quad (2)$$

$$\partial_t T + \mathbf{u} \cdot \nabla T = \kappa \nabla^2 T, \quad (3)$$

where $\mathbf{g} = (0, 0, -g)$ is the gravity acceleration, ν and κ are the kinematic viscosity and diffusivity respectively. The initial condition for the velocity at position $\mathbf{r} = (x, y, z)$ is $\mathbf{u}(\mathbf{r}, 0) = 0$, while for the temperature field $T(\mathbf{r}, 0) = T_0(z)$ we consider a generic power-law distribution given by (1). The only inviscid dimensional parameter that relates small spatial and temporal scales is $\xi = \beta g \theta_0 / L^c [\ell^{1-c} / t^2]$. Thus, for the box of size

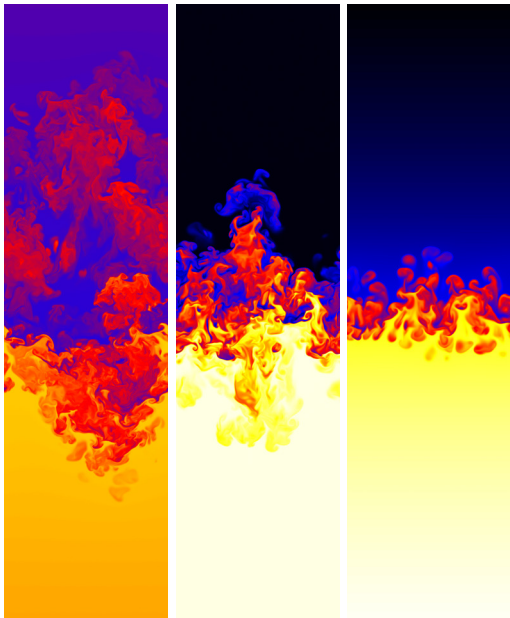


FIG. 1. (Color online). Snapshots of the vertical section of the temperature field T for three simulations of RT turbulence with power law initial condition (1) with $c = -0.25$ (left), $c = 0$ (center) and $c = 0.25$ (right) at time $t = 4t_*$. High (low) temperature is represented by yellow (blue).

L , the corresponding integral temporal scale is given by $t_* = \xi^{-1/2} L^{(1-c)/2} = \sqrt{L/(\beta g \theta_0)}$. The distribution (1) is unstable and the dimensional argument provides the inviscid growth rate $\lambda \simeq \xi^{1/2} k^{(1-c)/2}$ for the modes with wavenumber k , where the dimensionless proportionality coefficient can be determined by solving the linearized problem [21]. This dispersion relation predicts explosive instability at small scales for all $c < 1$.

The nonlinear development of the RT instability produces a mixing zone of width $h(t)$. Its evolution can be determined on dimensional grounds [22–24] from (1) and (2) in the form

$$u(t)^2/h(t) \simeq \beta g \theta_0 (h(t)/L)^c, \quad (4)$$

where $u(t)$ is a large-scale velocity. Assuming that $u \simeq dh/dt$, one ends with

$$h(t) \simeq L \left(\frac{t}{t_*} \right)^{\frac{2}{1-c}}, \quad u(t) \simeq U \left(\frac{t}{t_*} \right)^{\frac{1+c}{1-c}}, \quad (5)$$

where $U = L/t_*$ and t_* was defined above. Notice that the first expression can be reinterpreted as a standard RT diffusion

$$h(t) = \alpha_c \mathcal{A}_c(t) g t^2 \quad (6)$$

where $\mathcal{A}_c(t) = (\beta \theta_0)^{1/(1-c)} (g t^2/L)^{c/(1-c)}$ is the time dependent Atwood number and the pre-factor α_c represents the generalization of the standard RT α coefficient [25].

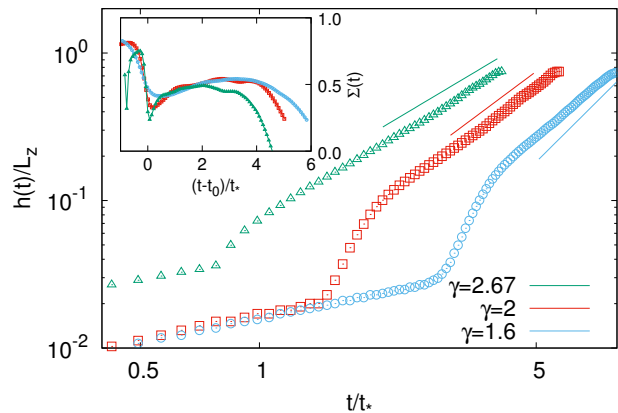


FIG. 2. Temporal evolution of the mixing layer $h(t)$. From left to right: $c = -0.25$ (green triangles), $c = 0$ (red squares) and $c = 0.25$ (blue circles). The three lines represent the power law predicted by the formula (5) with $\gamma = 2/(1-c)$. Inset: Efficiency of kinetic energy production $\Sigma = -(dE/dt)/(dP/dt)$ as a function of time for the three cases $c = -0.25$ (green triangles), $c = 0$ (red squares) and $c = 0.25$ (blue circles).

In order to test the above predictions, we performed direct numerical simulations (DNS) of the system of equations (2–3) in a periodic domain of size with $L_y = L_x$ and $L_z = 4L_x$ by means of a fully parallel pseudo-spectral code at resolution $512 \times 512 \times 2048$ for initial conditions (1) with different c . For all runs we have $\beta g = 1/2$, $\theta_0 = 1$ and $\text{Pr} = \nu/\kappa = 1$. RT instability is seeded by adding to the initial density field a white noise of amplitude $10^{-3}\theta_0$ and statistical quantities are averaged over 10 independent runs. Figure 1 shows examples of the vertical section of the temperature field for three different initial conditions taken at the same computational time. We estimate the width $h(t)$ of the ML on the basis of the mean temperature profile $\bar{T}(z, t) = \int T(x, y, z, t) dx dy$ as the region on which $|\bar{T}(z, t) - \bar{T}(z, 0)| > \delta \theta_0$ with $\delta = 5 \times 10^{-3}$ [26]. In Fig. 2 we show that the evolution of $h(t)$ is in good agreement with the power law predicted by scaling (6) for the three different values of c . A small deviation is observed for the largest c (which corresponds to the faster growth) probably because of the short range of temporal scaling. This results confirms that the balance (4) gives the correct evolution of the mixing layer, even over non-uniform backgrounds.

Equation (4) represents the conversion of available potential energy, $P(t) = -\beta g \int z \bar{T}(z, t) dz$ into turbulent kinetic energy $E(t) = (1/2) \langle \mathbf{u}(\mathbf{r}, t)^2 \rangle$ where with $\langle \bullet \rangle$ we intend the integral over the whole volume. Part of potential energy is dissipated by viscosity, as the energy balance from (2-3) reads $-dP/dt = \beta g \langle wT \rangle = dE/dt + \varepsilon_\nu$, where $\varepsilon_\nu = \nu \langle (\nabla \mathbf{u})^2 \rangle$. It is therefore interesting to measure the efficiency of the production of turbulent fluctuations,

defined as [27, 28]

$$\Sigma = -\frac{dE/dt}{dP/dt} \quad (7)$$

and to check how this is affected by the initial distribution. The inset of Fig. 2 shows the time evolution of Σ , (for clarity shifted by the time t_0 needed for the onset of the self-similar growth) for the three different cases. The indication is that the efficiency of conversion of potential energy into kinetic energy is independent on the initial density profile.

To have control on local quantities, we studied the evolution equation for the mean temperature profile:

$$\partial_t \bar{T} + \partial_z \bar{w} \bar{T} = \kappa \partial_{zz}^2 \bar{T}. \quad (8)$$

Using a Prandtl Mixing Layer first-order closure with homogeneous eddy diffusivity $K(t)$, the heat transfer is related to the local temperature gradient by [29]:

$$\bar{w} \bar{T} = -K(t) (\partial_z \bar{T} - c \bar{T}/z). \quad (9)$$

In the above expression, the correction term $c \bar{T}/z$ ensures that $\bar{w} \bar{T}$ vanishes outside the mixing zone, where \bar{T} is given by Eq. (1). Neglecting the viscous term, equation (14) can be recast into

$$\partial_t \bar{T} = K(t) \partial_z (\partial_z \bar{T} - c \bar{T}/z). \quad (10)$$

The effective diffusivity is expected to depend on time as uh , leading to $K(t) = b_c LU(t/t_*)^{(3+c)/(1-c)}$ with a free dimensionless parameter b_c . In this case a self-similar solution of (16) is obtained in the form (see Supplemental Material [30])

$$\bar{T}(z, t) = -\theta_0 \left(\frac{|z|}{L} \right)^c f_c(\eta), \quad \eta = \frac{z}{L} \frac{(t/t_*)^{-\frac{2}{1-c}}}{\sqrt{(1-c)b_c}}, \quad (11)$$

where the function

$$f_c(\eta) = \frac{2 \operatorname{sgn}(\eta)}{\Gamma(\frac{1-c}{2})} \int_0^{|\eta|} x^{-c} e^{-x^2} dx \quad (12)$$

is such that $f_c \rightarrow \pm 1$ as $\eta \rightarrow \pm\infty$. For $c = 0$ (standard RT), the solution reduces to the error function $f_0(\eta) = \operatorname{erf}(\eta)$ which is known to be a good fit for standard RT evolution [29]. In Fig. 3 we show that the homogeneous Prandtl approach works well also for $c \neq 0$ by plotting the rescaled temperature profiles, for the three different c 's considered, at three times as function of the rescaled coordinate η , as given by (18), superposed with the solution (26).

RESULTS FOR SHELL MODELS. The described phenomena can be also observed with high accuracy in a shell model for the RT evolution introduced in [20]. This system defines the dynamics at discrete vertical scales

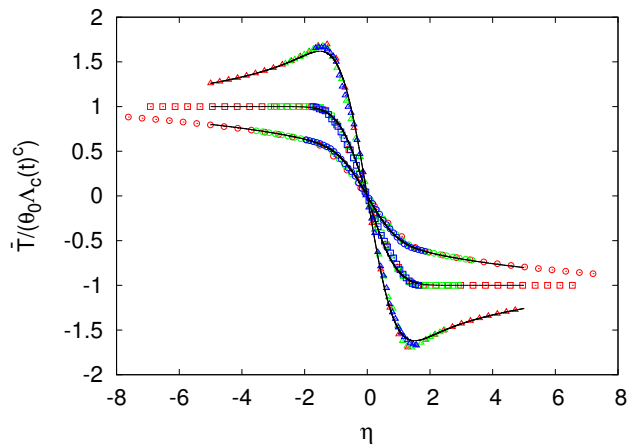


FIG. 3. Rescaled temperature profiles $\bar{T}/(\theta_0 \Lambda_c(t)^c)$ averaged over ten independent runs *vs* the vertical coordinate η (18), for $c = 0$ (squares), $c = 0.25$ (circles) and $c = -0.25$ (triangles) at three different times (in red the earliest, in blue the latest). $\Lambda_c(t) = \sqrt{(1-c)b_c(t/t_*)^{2/(1-c)}}$ is the time scaling factor of η in (18). The fitting parameters are: $b_0 = 6 \times 10^{-5}$, $b_{0.25} = 1.2 \times 10^{-6}$ and $b_{-0.25} = 7 \times 10^{-4}$. The solid lines represent the function $-|\eta|^c f_c(\eta)$, with $f_c(\eta)$ given by equation (26).

(“shells”) $z_n = 2^{-n}L$ with $n = 1, 2, \dots$, where the associated variables ω_n , R_n and T_n describe vorticity, horizontal and vertical temperature fluctuations, respectively. We modified the equations described in [20] by using the complex nonlinearity of the Sabra model [31, 32] (see Supplemental Material [30]). The shell model retains all most important scaling properties, symmetries and invariants of the original Boussinesq equations (2–3). At $t = 0$, the analogue of initial conditions (1) must be chosen with vanishing vorticity and horizontal temperature variations $\omega_n(0) = R_n(0) = 0$, while for the vertical temperature variables we choose

$$T_n(0) = i\theta_0 \left(\frac{z_n}{L} \right)^c \quad (13)$$

for all n . This initial condition leads to the same explosive dispersion relation $\lambda_n = \xi^{1/2} k_n^{(1-c)/2}$ as the full model (1–3) (see Supplemental Material [30]). Phenomenological theory of the RT instability for the shell model is essentially identical to the one of the full 3D system [23], with turbulent fluctuations propagating from small to large scales. It is convenient to characterize the size of the ML with the expression $h(t) = \sum |T_n(t)/T_n(0) - 1| z_n$, which estimates the largest scale z_n at which the temperature profile $T_n(t)$ deviates from its initial value $T_n(0)$. This definition is in spirit of the commonly used integral formulas for the ML width [7].

By performing a large number of simulations with small dissipative coefficients $\nu = \kappa = 10^{-10}$ and tiny random initial perturbations at small scales, we accurately verify the scaling law (5) for $c = -0.25, 0, 0.25, 0.5, 0.7$ in Fig. 4, where solid lines represent the numerical results

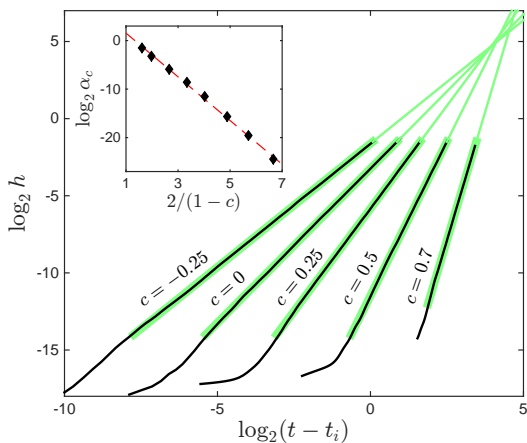


FIG. 4. Log-log growth of $h(t)$ in the shell model for different exponents c . The parameters L , βg and θ_0 were set to unity. The statistics was obtained from 10^3 evolutions, where a small random perturbation was added to the variables R_n at shells $n \geq 16$. Inset: pre-factor α_c vs c , fitted with the straight dashed line.

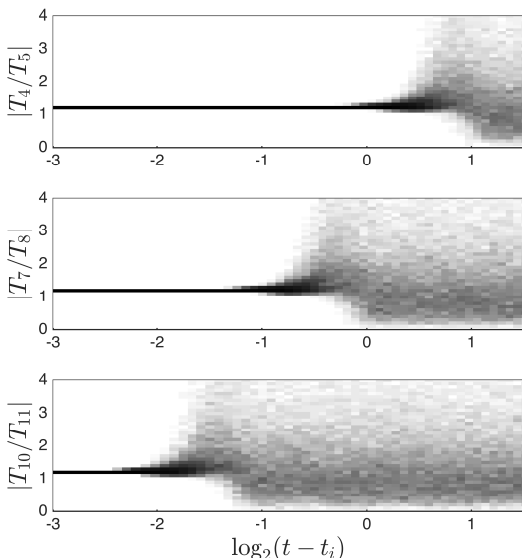


FIG. 5. PDFs (darker color for larger probability) for the ratios of temperature variables $|T_n/T_{n+1}|$ as functions of time: $n = 4$ (upper), $n = 7$ (middle) and $n = 10$ (lower) panels in the case $c = 0.25$.

(averaged over realizations) and the green lines show the theoretical prediction. Here we use the small time shift t_i accounting for the small initialization time, which improves the comparison.

The results in Fig. 4 provide with high accuracy the dimensionless pre-factor α_c for the power-law growth of the ML, see Eqs. (5-6). Dependence of this pre-factor on the singularity exponent c can be fitted well with the formula $\alpha_c \approx \alpha_L \alpha_t^{-2/(1-c)}$ as shown by the inset in Fig. 4. The quantities α_L and α_t have a simple physical meaning: they define the dimensional length and time scales, $\tilde{L} =$

$\alpha_L L$ and $\tilde{t} = \alpha_t t_*$, which reduce the ML width expression to the universal form, $h(t)/\tilde{L} = (t/\tilde{t}_*)^{2/(1-c)}$. Thus, the ML reaches the size \tilde{L} at the time \tilde{t} independently of the singularity exponent c ; this fact can be seen in Fig. 4 as an (approximately) common intersection point of the green lines. In the limit $c \rightarrow 1$ (constant temperature gradient with no singularity), the graph $h(t)$ approaches the vertical line at time \tilde{t} , which means that unstable modes at all scales get excited simultaneously.

It is argued [18, 19] that spontaneous stochastic turbulent fluctuations develop in the inverse cascade from small to large scales. In the RT turbulence, existence of such a cascade must reflect in the stochastic growth of the mixing layer independently of the intensity of the initial perturbation similarly to what happens in the turbulent Richardson dispersion describing the evolution of pairs of Lagrangian tracers [33]. Such phenomenon can be conveniently studied with the renormalized (logarithmic) space-time coordinates: $-n = \log_2 z_n$ and $\tau = \log_2(t - t_i)$. To highlight the stochastic aspect, we choose to measure the probability distribution function of the ratios among temperature fluctuations at adjacent shells, $|T_n/T_{n+1}|$, which are the equivalent of velocity multipliers used in cascade description of fully developed turbulence [34, 35]. Figure 5 presents the time-dependent PDFs obtained numerically in the case $c = 0.25$ starting from many initial conditions different by a very small perturbation. These results support the idea that the ML growth can be mapped to a stochastic wave in appropriate renormalized variables $(-n, \tau)$. The wave speed is constant and given by the exponent $2/(1-c)$ of ML width from Eq. (5). Such a wave represents a front of the turbulent fluctuations, which propagates into a deterministic left state (delta function PDF) corresponding to the rough initial background (30), and leaves behind the stationary turbulent state on the right. This description naturally explains the universality of the ML evolution and its spontaneously stochastic behavior in the inertial range [20, 36].

CONCLUSIONS. We have studied numerically and analytically Rayleigh-Taylor turbulence with a non-uniform singular initial background. We have shown that independently of the singularity exponent, the asymptotic self-similar growth of the ML is universal, if properly renormalized, i.e. by looking at the mixing efficiency and at the mean rescaled Temperature profile. We show that a closure model based on the Prandtl mixing layer approach is able to reproduce analytically the time evolution of the mean temperature profiles. By using a shell model we have provided numerical data supporting the above findings also at much larger resolution both in time and scales. Finally, we have shown that RT evolution can be reinterpreted in terms of the phenomenon known as *spontaneous stochasticity* where the growth of the mixing layer is mapped into the propagation of a wave of

turbulent fluctuations on a rough background.

ACKNOWLEDGEMENTS. L.B. acknowledges financial support from the European Unions Seventh Framework Programme (FP7/2007-2013) under Grant Agreement No. 339032. A.A.M. was supported by the CNPq Grant No. 302351/2015-9. G.B. acknowledges financial support by the project CSTO162330 *Extreme Events in Turbulent Convection*. HPC center CINECA is gratefully acknowledged for computing resources.

-
- [1] D.H. Sharp, *Physica D* **12**, 1 (1984).
 [2] H.J. Kull, *Phys. Rep.* **206**, 197 (1991).
 [3] S.I. Abarzhi, *Phil. Trans. Roy. Soc. London A* **1916**, 1809 (2010).
 [4] G. Boffetta and A. Mazzino, *Annu. Rev. Fluid Mech.* **49**, 119 (2017).
 [5] Y. Zhou, *Phys. Rep.* **720**, 1 (2017).
 [6] M. Zingale, S.E. Woosley, C.A. Rendleman, M.S. Day and J.B. Bell, *Astrophys. J.* **632**, 1021 (2005).
 [7] W.H. Cabot and A.W. Cook, *Nat. Phys.* **2**, 562-569 (2006).
 [8] J. Bell, M. Day, C. Rendleman, S. Woosley, M. Zingale *Astrophys. J.* **608**, 883 (2004).
 [9] M.C. Kelley, G. Haerendel, H. Kappler, A. Valenzuela, B.B. Balsley, D.A. Carter, W.L. Ecklund, C.W. Carlson, B. Häusler and R. Torbert, *Geophys. Res. Lett.* **3**, 448-450 (1976).
 [10] R.P. Taleyarkhan, C.D. West, J.S. Cho, R.T. Lahey Jr., R.I. Nigmatulin and R.C. Block, *Science* **295**, 1868-1873.
 [11] J.D. Lindl, *Inertial Confinement Fusion*. Springer-Verlag, New-York, (1998).
 [12] G. Dimonte, P. Ramaprabhu and M. Andrews, *Phys. Rev. E* **76**, 046213 (2007).
 [13] G. Dimonte and M. Schneider, *Phys. Rev. E* **54**, 3740 (1996).
 [14] D. Livescu, T. Wei and M.L. Petersen, *J. Phys.: Conf. Ser.* **318**, 082007 (2011).
 [15] A.S. Monin and A.M. Obukhov, *Trudy Geofiz. Inst. Akad. Nauk SSSR* **24**, 163-187 (1954).
 [16] B.A. Kader and A.M. Yaglom, *J. Fluid Mech.* **212**, 637-662 (1990).
 [17] L. Biferale, F. Mantovani, M. Sbragaglia, A. Scagliarini, F. Toschi and R. Tripiccone, *Phys. Rev. E* **84**, 016305 (2011).
 [18] C.E. Leith and R.H. Kraichnan, *J. Atm. Sci.* **29**, 1041 (1972).
 [19] G.L. Eyink, *J. Stat. Phys.* **83**, 955 (1996).
 [20] A.A. Mailybaev, *Nonlinearity* **30**, 2466 (2017).
 [21] S. Chandrasekhar, *Hydrodynamic and hydromagnetic stability*. Courier Corporation, (2013).
 [22] A.W. Cook and P.E. Dimotakis, *J. Fluid Mech.* **443**, 69-99 (2001).
 [23] M. Chertkov, *Phys. Rev. Lett.* **91**, 115001 (2003).
 [24] J.R. Ristorcelli and T.T. Clark, *J. Fluid Mech.* **507**, 213-253 (2004).
 [25] G. Dimonte et al, *Phys. Fluids* **16**, 1668-1693 (2004).
 [26] S.B. Dalziel, P.F. Linden and D.L. Youngs, *J. Fluid Mech.* **399**, 1 (1999).
 [27] G. Boffetta, A. Mazzino, S. Musacchio and L. Vozella

Phys. Fluids **22**, 035109 (2010).

- [28] G. Boffetta, A. Mazzino and S. Musacchio *Phys. Rev. Fluids* **1**, 054405 (2016).
 [29] G. Boffetta, F. De Lillo and S. Musacchio, *Phys. Rev. Lett.* **104**, 034505 (2010).
 [30] See Supplemental Material.
 [31] V.S. Lvov, E. Podivilov, A. Pomyalov, I. Procaccia and D. Vandembroucq, *Phys. Rev. E* **58**, 1811 (1998).
 [32] L. Biferale, *Annual Rev. Fluid Mech.* **35**, 441 (2003).
 [33] G. Falkovich, K. Gawdzki, and M. Vergassola, *Rev. Mod. Phys.* **73**, 913 (2001).
 [34] R. Benzi, L. Biferale and G. Parisi, *Physica D* **65**, 163 (1993).
 [35] Q. Chen, S. Chen, G.L. Eyink and K.R. Sreenivasan, *Phys. Rev. Lett.* **90**, 254501 (2003).
 [36] A.A. Mailybaev, *Nonlinearity* **29**, 2238 (2016).

SUPPLEMENTAL MATERIAL

Derivation of the mean profile solution, $\bar{T}(z, t)$

The equation for the mean temperature profile

$$\partial_t \bar{T} + \partial_z \bar{w} \bar{T} = \kappa \partial_{zz}^2 \bar{T}, \quad (14)$$

with the following closure for the turbulent heat flux

$$\bar{w} \bar{T} = -K(t) (\partial_z \bar{T} - c \bar{T}/z), \quad (15)$$

becomes

$$\partial_t \bar{T} = K(t) \partial_z (\partial_z \bar{T} - c \bar{T}/z). \quad (16)$$

Let us write (16) as

$$\partial_t \bar{T} = K(t) \partial_z \left[|z|^c \partial_z \left(\frac{\bar{T}}{|z|^c} \right) \right]. \quad (17)$$

Substituting for \bar{T} the ansatz

$$\bar{T}(z, t) = -\theta_0 \left(\frac{|z|}{L} \right)^c f_c(\eta) \quad (18)$$

and dropping the common factor $-\theta_0 (|z|/L)^c$ yields

$$\partial_t f_c = \frac{K(t)}{|z|^c} \partial_z (|z|^c \partial_z f_c), \quad (19)$$

where $f_c = f_c(\eta)$ and η is given by

$$\eta(z, t) = \frac{1}{\sqrt{(1-c)b_c}} \frac{z}{L} \left(\frac{t}{t_*} \right)^{-\frac{2}{1-c}}. \quad (20)$$

We can write Eq. (19) in the form

$$\frac{df_c}{d\eta} \partial_t \eta = K(t) \left(\frac{c}{z} \frac{df_c}{d\eta} + \frac{d^2 f_c}{d\eta^2} \partial_z \eta \right) \partial_z \eta. \quad (21)$$

Using (20) and the definition of

$$K(t) = b_c \frac{L^2}{t_*} \left(\frac{t}{t_*} \right)^{(3+c)/(1-c)} \quad (22)$$

in Eq. (21) leads, after a long but elementary derivation, to:

$$\frac{d^2 f_c}{d\eta^2} + \left(\frac{c}{\eta} + 2\eta\right) \frac{df_c}{d\eta} = 0. \quad (23)$$

Denoting $g_c = df_c/d\eta$ we can recast the above expression in to:

$$\frac{dg_c}{d\eta} + \left(\frac{c}{\eta} + 2\eta\right) g_c = 0. \quad (24)$$

The general solution of Eq. (24) has the form

$$g_c(\eta) = C|\eta|^{-c} e^{-\eta^2} \quad (25)$$

with an arbitrary pre-factor C . Finally, the solution for $f_c(\eta) = \int g_c(\eta) d\eta$ takes the form

$$f_c(\eta) = \frac{2 \operatorname{sgn}(\eta)}{\Gamma\left(\frac{1-c}{2}\right)} \int_0^{|\eta|} x^{-c} e^{-x^2} dx \quad (26)$$

where the factor $C = 2/\Gamma\left(\frac{1-c}{2}\right)$ is determined from the condition $f_c \rightarrow \pm 1$ as $\eta \rightarrow \pm\infty$.

Shell Model for RT evolution

We introduce the RT shell model equations in the form

$$\begin{aligned} \dot{\omega}_n = & -\omega_{n+2}\omega_{n+1}^*/4 + \omega_{n+1}\omega_{n-1}^*/2 \\ & + 2\omega_{n-1}\omega_{n-2} + i\beta g R_n/z_n - \nu\omega_n/z_n^2, \end{aligned} \quad (27)$$

$$\dot{R}_n = \omega_n^* R_{n+1} - \omega_{n-1} R_{n-1} + \omega_n T_n^* - \kappa R_n/z_n^2, \quad (28)$$

$$\dot{T}_n = \omega_n^* T_{n+1} - \omega_{n-1} T_{n-1} - \omega_n R_n^* - \kappa T_n/z_n^2. \quad (29)$$

This system defines the dynamics at discrete vertical scales (“shells”) $z_n = 2^{-n}L$ with $n = 1, 2, \dots$, where the

associated variables ω_n , R_n and T_n describe vorticity, horizontal and vertical temperature fluctuations, respectively. The integral scale is usually chosen as $L = 1$.

Equations (27-29) are analogous to those proposed in [20], except for the fact that here we used the more popular Sabra model nonlinearity [31, 32] for the vorticity Eq. (27), where $\omega_n = u_n/z_n$ and u_n are the velocity shell variables for the Sabra model. Notice that usually in shell model literature the equations are written using $k_n = 1/z_n$ to denotes scales in Fourier space. Equation (27) without the buoyancy term has energy $E = \sum |u_n|^2$, and the helicity $H = \sum (-1)^n |u_n \omega_n|$ as inviscid invariants in agreement with 3D Navier-Stokes equations. Equations (28) and (29) possess the inviscid invariant $S = \sum |R_n|^2 + |T_n|^2$, which can be interpreted as the entropy.

One can show that the initial condition

$$T_n(0) = i\theta_0 \left(\frac{z_n}{L}\right)^c \quad (30)$$

with vanishing $\omega_n(0) = R_n(0) = 0$ leads to the exponentially growing modes [20]. Let us consider small perturbations, $\Delta\omega_n$ and ΔR_n , and neglect the dissipative terms. Then, Eqs. (27) and (28) linearized near the initial state read

$$\Delta\dot{\omega}_n = \frac{i\beta g}{z_n} \Delta R_n, \quad \Delta\dot{R}_n = -i\theta_0 \left(\frac{z_n}{L}\right)^c \Delta\omega_n. \quad (31)$$

Solution of these equations provide one unstable mode for each “wavenumber” $k_n = 1/z_n$ with the corresponding positive Lyapunov exponent

$$\lambda_n = \xi^{1/2} k_n^{(1-c)/2}, \quad \xi = \beta g \theta_0 / L^c, \quad (32)$$

in the direct analogy with the RT instability of the full 3D system.